ISTITUTO NAZIONALE DI FISICA NUCLEARE

Sezione di Milano

INFN/TC-95/23
23 Agosto 1995

F. Broggi, D. Pedrini, L. Rossi:

THERMAL CONDUCTIVITY MEASUREMENTS AT CRYOGENIC TEMPERATURES AT L.A.S.A.

SIS-Pubblicazioni
dei Laboratori Nazionali di Frascati

INFN - Istituto Nazionale di Fisica Nucleare
Sezione di Milano

INFN/TC–95/23
23 Agosto 1995

THERMAL CONDUCTIVITY MEASUREMENTS AT CRYOGENIC TEMPERATURES AT L.A.S.A.

F. Broggi, D. Pedrini, L. Rossi

INFN–Sezione di Milano, Via Celoria 16, I–20133 Milano, Italy
Laboratorio LASA, Via Fratelli Cervi 201, I – 20090 Segrate

Abstract

In a previous report the experimental apparatus for measuring the thermal conductivity of coil blocks and composite materials has been widely decribed. Here we describe the improvement realized to have better control of the reference junction temperature and the measurements carried out on Nb_3Sn cut out from 2 different coils (named LASA3 and LASA5), showing the difference between the longitudinal and the transverse thermal conductivity. Two different methods of data analysis are presented, the "Derivative Approximated Method (DAM) and the "Thermal Conductivity Integral" (TCI). The data analysis for the tungsten and the LASA5 coil has been done according to the two methods showing that the TCI method with polynomial functions is not adequate to describe the thermal conductivity. Only a polynonial fit based on the TCI method but limited at a lower order than the nominal, when the data are well distributed along the range of measurements, can describe reasonably the thermal conductivity dependence with the temperature. Finally the measurements on a rod of BSCCO 2212 high T_c superconductor are presented.

1 INTRODUCTION

Magnetic fields in the range 10 to 20 Tesla by means of superconducting magnets are nowadays available. Nevertheless the problems of reliable operation and of protection in case of quench is still open and under investigation. This is especially true when very high fields, B $\geq$ 15 Tesla, are reached by means of superconducting coupled adiabatic coils[1][2] [3]. In fact the use of fully epoxy impregnated coils wound with cable with small amounts of copper (or without) is very effective in cost saving but can result in poor protection of the magnet in case of quench and several papers have been published about the quench propagation[4][5]. In our lab a numerical code, describing the quench propagation in adiabatic, multicoil, multisection magnets has been developed [6].

It has been shown[4][5] that in an adiabatic magnet the transverse propagation, i.e. turn to turn and layer to layer, is the dominant mechanism of the quench propagation. While the longitudinal propagation, along the cable, is dominated by heat diffusion through the metal, the transverse one is mainly determined by the heat diffusion through the insulation.

The longitudinal velocity of the normal zone propagation, v_l, can be analytically derived and the transverse velocity v_t is usually given as :

$$v_t = v_l \times \sqrt{\lambda_t / \lambda_l}$$

where λ_l and λ_t are the longitudinal and transverse thermal conductivities of the winding. This simple expression can be modified, according to[7], to take into account the fact that heat does not diffuse significantly into the resin in the longitudinal propagation but it does so in the transverse one. The importance of the effective thermal conductivity of the winding is evident in the above formula.

The values of λ_l can be fairly well calculated, both as a function of temperature and magnetic field. Indeed it involves only properties of metals, mainly of the copper. Even in the case of a small percentage of copper, or no copper at all, λ_l can be calculated with a reasonable degree of accuracy by considering all the metals of the cable acting as thermal conductances in parallel.

Very different considerations apply to the evaluation of λ_t. Wires for high field magnets are generally composed of Nb_3Sn or $(NbTa)_3Sn$ filaments embedded in a CuSn matrix and generally the stabilizing copper is protected by a thin barrier made out of tantalum or other suitable materials and a simple model based on parallel or series of thermal conductances is not reliable. The situation is more complicated for multistrand cables, where the interstrand contacts can give a non negligible contribution to the transverse heat conduction, even if the twist of the cable can reduce the importance of the interstrand thermal contacts.

Even if λ along the cross section of the cable can be computed, one must still evaluate λ through the insulation, the most relevant parameter. The insulation is generally either glass braid (or tape) or, for NbTi single wire, a thin coating of varnish (such as formvar). After casting of the coil with epoxy resin, in the case of glass insulation one has a composite whose properties are very similar to the properties of G10 or G11 fiber glass composite. In case of formvar insulation the thermal properties of formvar-epoxy composite are considered be similar to the ones of the epoxy resin.

The thermal conductivity of the resin- glass fibre composite is not so easy to predict as it is for the metals and different values are given in the literature[8][9] and in the case of a composite like epoxy - glass braid the relative cross section of every component is difficult to determine and depends on the considered directions (anisotropy). Moreover, another source of uncertainty is given by the effective thermal transmission between the metal and the insulation, because the surface conditions can strongly affect the quality of bonding between the different elements, with possible non negligible surface thermal resistance.

We started an experimental program aiming to build a thermal conductimeter dedicated to measurements on coil blocks, cut out from real windings, and on composite materials. In this

conductimeter it is possible to measure samples under a compression force up to 3 KN, and the temperature can range between 2 and 350 K. It is possible, with minor modifications, to insert the apparatus inside the room temperature bore of an 8 tesla superconducting magnet.

2 THEORY OF MEASUREMENT

2.1 The Derivative Approximation Method (DAM)

The thermal conductivity of the solids spans over a range of 5 order of magnitude, depending on the temperature and on the material considered, and many different methods can be used to measure the thermal conductivity. They can be divided in two classes, the steady-state and the dynamic methods [10, 11]. In the steady state methods the heat flows into in the sample and, at the equilibrium, the measurement of the sample temperature profile and of the power allow the determination of the thermal conductance. Eventually from the geometry the conductivity can be evaluated. In the dynamic methods the thermal conductivity is deduced by a measurement of the diffusivity of the sample, by measuring the time evolution of the temperature profile along the sample. We measured the thermal conductivity with the absolute steady state method of the axial heat flow. According to this method the heat flows unidimensionally along the sample. From the Fourier - Biot law follows:

$$\lambda(T) = -\frac{\dot{Q}}{S}\frac{dl}{dT} \tag{1}$$

replacing dl/dT with $L/\Delta T$ and considering S as a constant we get

$$\lambda = -\frac{\dot{Q}L}{S\ \Delta T} \tag{2}$$

Here we make the approximation $dl/dT \simeq L/\Delta T$. The determination of the thermal conductivity according to this hypotesis is referred as DAM. More precisely the relation (2) follows by integration of (1) between T_1 and T_2:

$$\int_{T_1}^{T_2} \lambda(T)\ dT = -\dot{Q}\int_0^L \frac{1}{S}dl \tag{3}$$

The thermal conductivity determined by this method is the mean value of the conductivity in the temperature range T_1, T_2, in fact the integration of the (2) gives, assuming S as a constant,

$$\int_{T_1}^{T_2} \lambda(T)\ dT = \int_{T_1}^{T_2} -\frac{\dot{Q}\ dl}{S\ dT}\ dT = -\frac{\dot{Q}\ L}{S} \tag{4}$$

So, dividing by $\Delta T = T_2 - T_1$ we get:

$$\bar{\lambda} \equiv \frac{1}{\Delta T}\int_{T_1}^{T_2} \lambda(T)dT = -\frac{\dot{Q}L}{S\ \Delta T} \tag{5}$$

For the theorem of the mean value

$$\int_{T_1}^{T_2} \lambda(T)\ dT = \lambda(T^*)(T_2 - T_1) \tag{6}$$

where $T^* \in (T_2 - T_1)$, so

$$\bar{\lambda}(T_1, T_2) = \lambda(T^*) \tag{7}$$

We assume that the point T^* is exactly the mean value of T_1, T_2. i.e.

$$T^* = \bar{T} = \frac{T_1 + T_2}{2} \tag{8}$$

This assumption is exactly correct only if λ is constant with T or depends linearly on it. In all the other cases the assumption (7) leads to a relative error given by

$$\epsilon_{\lambda(\bar{T})} = \frac{\lambda(\bar{T}) - \bar{\lambda}(T_1, T_2)}{\bar{\lambda}(T_1, T_2)} \tag{9}$$

This error is intrinsic in the DAM method because of the $dl/dT \simeq L/\Delta T$ approximation. In general the smaller ΔT the more precise is the measurement of λ (being $\epsilon_{\lambda(\bar{T})} \to 0$ as $\Delta T \to 0$). Considering the experimental determination of λ, from the (2) affected only by errors on the temperatures T_1 and T_2, the relative error of the measurement is

$$\frac{\sigma_\lambda}{\lambda} = \frac{1}{\Delta T} \cdot \sqrt{(\sigma_{T_1})^2 + (\sigma_{T_2})^2} \tag{10}$$

where σ_{T_1} and σ_{T_2} are the errors on the determination of the temperature T_1 and T_2.

It is clear that this experimental error is high when ΔT is small, at fixed error σ_{T_1} and σ_{T_2}. Being the "intrinsic error" dependence on ΔT inverse respect to the "experimental error" one, the optimum ΔT for both the approximations is, combining the (9) and the (10),

$$\Delta T_{opt} = \frac{\dot{Q} \cdot L}{S \cdot \lambda(\bar{T})} - \sqrt{(\sigma_{T_1})^2 + (\sigma_{T_2})^2} = \frac{\sqrt{(\sigma_{T_1})^2 + (\sigma_{T_2})^2}}{\epsilon_{\lambda(\bar{T})}} \tag{11}$$

Studies on the error induced by the approximation (7) [12] showed that small temperature differences are needed only if λ is a rapid varying function of the temperature, or when the measurement occur at a phase transition, where λ is not continuous; in the other cases the DAM method used with temperature differences of some degrees lead to an error af about 1 - 2 %, because the thermal conductivity of most of the materials has a temperature dependence almost linear or constant over a range of some tens of degree. Care must be taken in determining the λ for pure metals between 30 and 40 K where λ has a maximum. Anyway the determination of the thermal conductivity for composed materials, like a coil block of a superconducting magnet, can be done with the DAM method because in this case we intend to measure the "mean", intended as global macroscopic, thermal conductivity, even if the λ of the single components (the superconductor, the insulation and the stabilizer) of a cable can differ each other of order of magnitude. The points obtained with the DAM are then plotted with a suitable function in order to have an analytical expression of the $\lambda = \lambda(T)$ on the desired temperature range.

2.2 The Thermal Conductivity Integral Method (TCI)

The TCI method allows the determination of λ without the limitation on the temperature intrinsic in the DAM method if an analytical representation of $\lambda(T)$ is known, or when $\lambda(T)$ can be described by an integrable function over the temperature range where the measurements are done. According to this method we suppose to represent the thermal conductivity as a power series of T:

$$\lambda(T) = \sum_{i=0}^{N-1} A_i T^i \tag{12}$$

with $T_{min} < T < T_{max}$, where T_{min} and T_{max} are the minimum and maximum temperature inside which the measurements are carried out. Being

$$\int_{T_1}^{T_2} \lambda(T)dT = -\frac{\dot{Q}}{S} \cdot L \tag{13}$$

by integrating the expression (12) we get

$$\sum_{i=1}^{N} A_i \frac{{T_2}^{i+1} - {T_1}^{i+1}}{i+1} = -\frac{\dot{Q}}{S} \cdot L \tag{14}$$

A set of N measurements of the experimental data $\dot{Q}$, L, S, T_1 and T_2 allows to calculate the coefficients A_i. If the maximum order of the power sum N is high, (N > 6), numerical problem can arise in the determination of the coefficients A_i. In order to overcome this problem it is possible to use the TCI method restricted to small temperature intervals and power series of order lower than 6. In the following sections the TCI method will be compared with the DAM one for two sets of experimental data (tungsten and Nb_3Sn). If the thermal conductivity is calculated with the TCI method at the mean temperature between T_{min} and T_{max}, the difference between the thermal conductivity determined with the DAM method is negligible. The functions obtained by the TCI method did not fit well the measurements giving an oscillating behaviour not in accordance to the thermal conductivity dependence on the temperature. The best results of the TCI were given when we had few measurements well distributed on the considered temperature range; anyway the results of the TCI analysis never looked better than the ones given by the DAM followed by a direct suitable fitting (see the section of data analysis).

3 DESCRIPTION OF THE MEASUREMENT APPARATUS

In a previous report [13] the conductimeter has been described with all the details, nevertheless for completeness we report in the following the description of the main features. The apparatus has been designed in order to measure the transverse thermal conductivity with the stationary method of the axial heat flux. The apparatus is basically constituted by 2 heat sinks at different temperatures; the sample is placed between them. The cold heat sink is at direct contact with the cryogenic fluid, while the warm one has an electric heater [14]. Two or more temperature sensors are placed along the sample, and, in stationary conditions, knowing the power flowing through the sample, the value of the thermal conductivity can be determined through the Fourier - Biot law.

$$\lambda(\bar{T}) \simeq \frac{\dot{Q}L}{S\,\Delta T} \tag{15}$$

In fig. 1 a section of the measurement apparatus is shown. The block of the material under measurement (the sample) is held between the copper heat sinks by a pressing system, in order to have a good thermal contact between the heat sinks and the sample. Measurements of the thermal conductivity at different values of clamping pressure are possible in case an evaluation of the effect of the thermal contact resistance is required.

The thermal contact between the heat sinks and the sample is improved by means of a special grease, containing a high percentage of tiny copper particles.

The pressing system and the support for the sample is a thermal conductance in parallel with the sample, so it has been designed in order to have a low conductance, to minimize the thermal losses from the sample to it (see fig. 1).

The pressing system consists of two G11 plates separated by 3 small nylon cylinders. The upper plate supports the heater, a copper block on wich the heating coil is wound. The junction between the G11 pressing plate and the heater is achieved through a hinge, that allowes a maximum

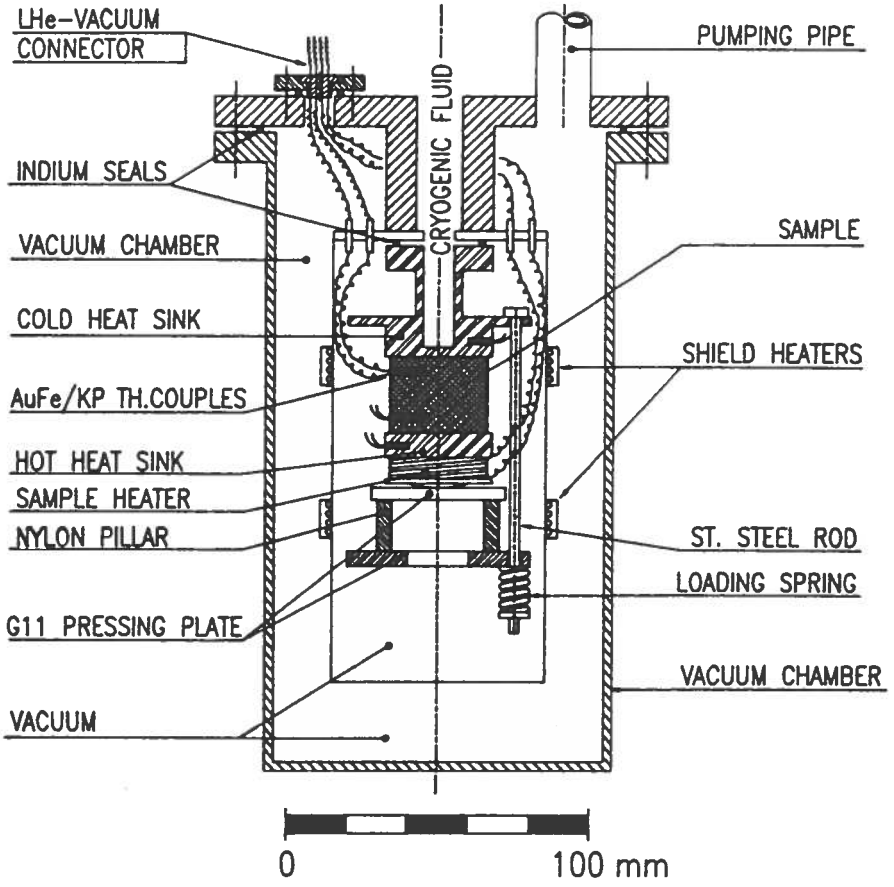

Figure 1: Sketch of the thermal conductimeter

angulation of about two degrees, and provides a good contact between the copper and the sample even if the two faces are not perfectly parallel. The lower G11 plate of the pressing system is connected to the upper part of the pressing system with 3 stainless steel rods. The clamping pressure can be varied by acting on the loading springs which compensate also the small differential thermal contraction between the stainless steel rods and the sample holder, so that the compression is almost constant at different temperatures.

All the system is enclosed in a gold plated stainless steel radiative shield, to minimize the radiative losses. Two heaters are placed on the radiative shield in order to generate a temperature profile similar to the temperature profile heater + the sample assembly. The flange where the radiative shield is attached has the feedthroughs for the thermocouples for the control signals and for the heaters: actually it is used as a reference junction for the thermocouples. The thermal sensors are AuFe(0.07% at.w.)-Cromel P thermocouples. This kind of sensors have been chosen for their easy use at low temperatures, small dimensions, low thermal capacity and because of its reliability in vacuum.

The system together with the radiation shield is enclosed in a vacuum chamber (made of stainless steel) which is maintained at a pressure of about 10^{-6} mbar by means of a turbomolecular pump, to avoid convective losses. The vacuum chamber is immersed in the cryogenic fluid. All the sealings of the flanges are indium rings. The maximum dimensions of a sample in the present arrangement are 35 mm diameter and 70 mm length, (but bigger sample size can be accomodated, especially if the thermal shield can be removed) and the measuring temperature range is 4.2 – 350 K[15]. Lower temperature measurements, down to 2 K can be available by pumping over the helium bath. In the photo (2) the conductimeter, without the thermal shield, with the sample of nbsn named LASA3 (see next sections) is shown.

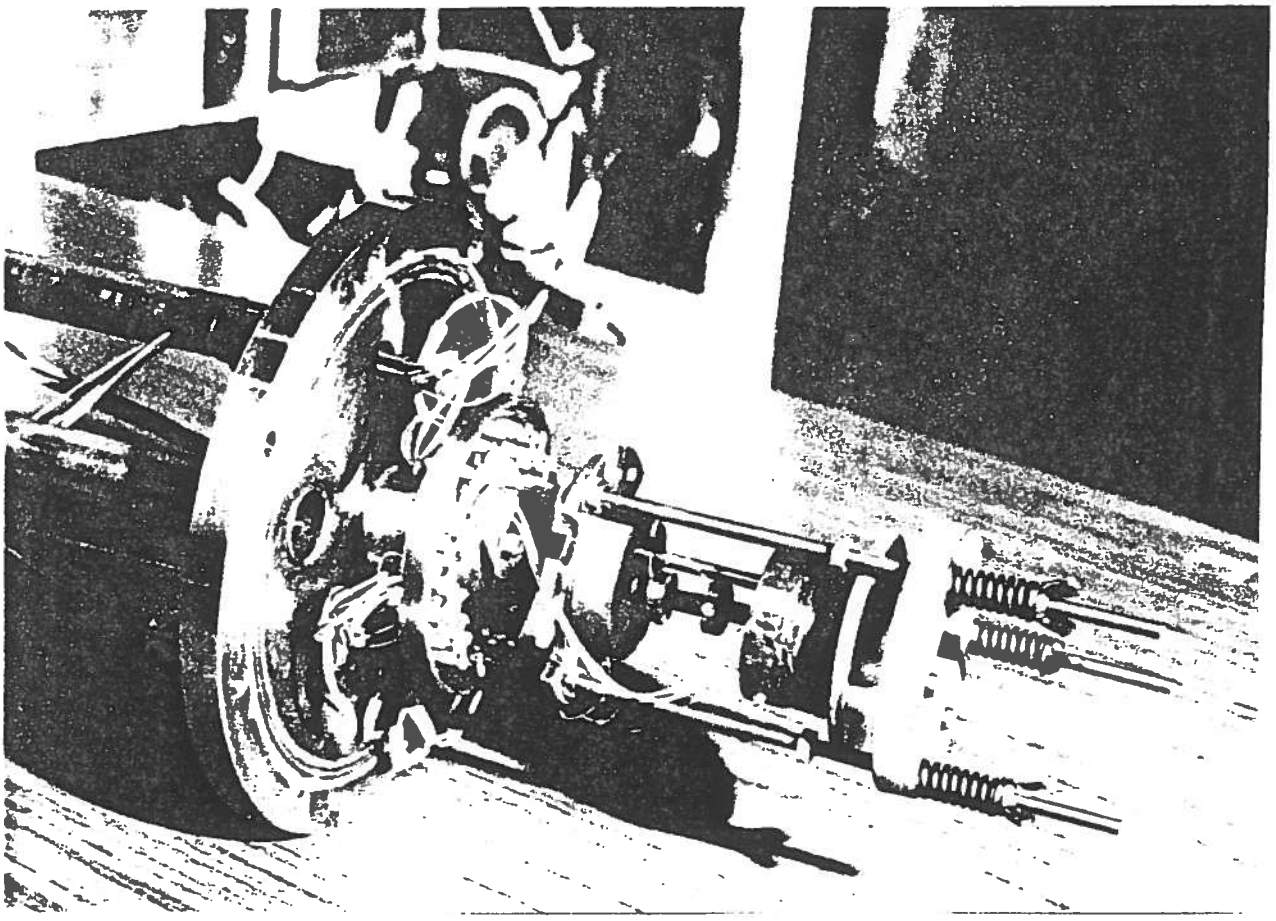

Figure 2: The conductimeter with the B1-2212 sample mounted.

3.1 The modification of the apparatus

The main modification has been the substitution of the flange were are the feedthroughs for the thermocouples. The old flange was in stainless steel and it has been substitute with one in copper. The modification was necessary because the cold reference junction of the thermocoules was not at a fixed temperature, when high power (about 1 W) were necessary for the measurements or when the heater of the shield were used. The drift of the temperature of the cold junction caused a lowering of the recorded temperature of the thermocouple attached at the cryogenic bath, lowering actually due to a local heating of the flange. The substitution of the flange with the copper one overcomes the problem, being the thermal conductivity of copper namely higher than that one of the stainless steel, thus avoiding the local heating. Conversely higher temperature of the thermocouple attached at the cryogenic bath has been registered, when high power was sent into the sample, and this was due to a real physical heating of the cryogen in a thin layer faced to the sample. In fact when the power is more than 1 W the transfer from metal to fluid enters in the "film boiling" regime with ΔT between metal and liquid of more than 1 K.

4 HEAT LOSSES IN THE SYSTEM

To evaluate the thermal conductivity we measure the temperature at the ends and in some points along the sample and the power dissipated by the heater. Actually the whole dissipated power will

not flow in the sample, but part of it will be lost through conduction in the supporting system, convection and radiation. The convective and radiative losses can be reduced to a negligible value by operating in vacuum and by the use of the radiative shield.

4.1 Conductive Losses

To describe the process we make use of the thermal conductance, defined from the Fourier - Biot law as

$$\dot{Q} = C\Delta T \qquad \rightarrow \qquad C = \frac{\dot{Q}}{\Delta T} = \bar{\lambda}(T_1, T_2)\frac{S}{L} \tag{16}$$

If the power flows thorough different materials its conductance will be

$$C = -\frac{\dot{Q}}{\Delta T} = \lambda_{eff}\frac{S}{L} \tag{17}$$

where λ_{eff} is the effective mean conductivity of the materials. The power flowing for conduction in the supporting system must be evaluated. The conductance of the supporting system is in parallel with the sample and its value must be carefully evaluated because it is not negligible when compared to the conductance of the sample made of insulating materials. To this aim the supporting system is described as a sequence of materials thermically connected in series and the power flowing through it is determined by its conductance $C = -\lambda_{eff}(S/L)_{eff}$. In this case the Fourier - Biot law cannot be directly integrated, without knowing the temperature profile along the supporting system. Once the temperature profile is known, the integration of $\lambda(T)$ can be done and the value of the conductance and of the mean conductivity can be determined.

Neglecting radiative and convective losses the temperature profile is determined by the continuity condition

$$\frac{d\dot{Q}}{dx} = 0 \tag{18}$$

That is

$$\frac{d}{dx}(\lambda(T)S(x)\frac{dT}{dx}) = 0 \tag{19}$$

That leads to the equation

$$\frac{d^2T}{dx^2} + \frac{1}{\lambda(T)}\frac{d\lambda(T)}{dT}(\frac{dT}{dx})^2 + \frac{1}{S(x)}\frac{dS(x)}{dx}\frac{dT}{dx} = 0 \tag{20}$$

With the boundary conditions

$$T(x = 0) = T_1 \qquad T(x = L) = T_2 \tag{21}$$

The solution of the equation cannot be analytically determined, being non linear and with variable coefficients; furthermore there is no analytical relation for the values of $\lambda(T)$, that are determined by a linear interpolation of experimental data. Therefore a numerical code has been developed in order to solve the equation (20) and to compare the "theoretical data" for C for a composite material (where the $\lambda(T)$ and $S(x)$ of each component is known) and the measured C.

In fig. 3 the conductance of the supporting system is plotted as a function of the mean temperature, between the heat sink and the heater. Two measurements of this conductive loss through the supporting system are shown too (dots in fig. 3).

The two calculated curves refer to different way of evaluating the sections of conduction of the various components of the supporting system. The "no-smoothing" line is determined considering

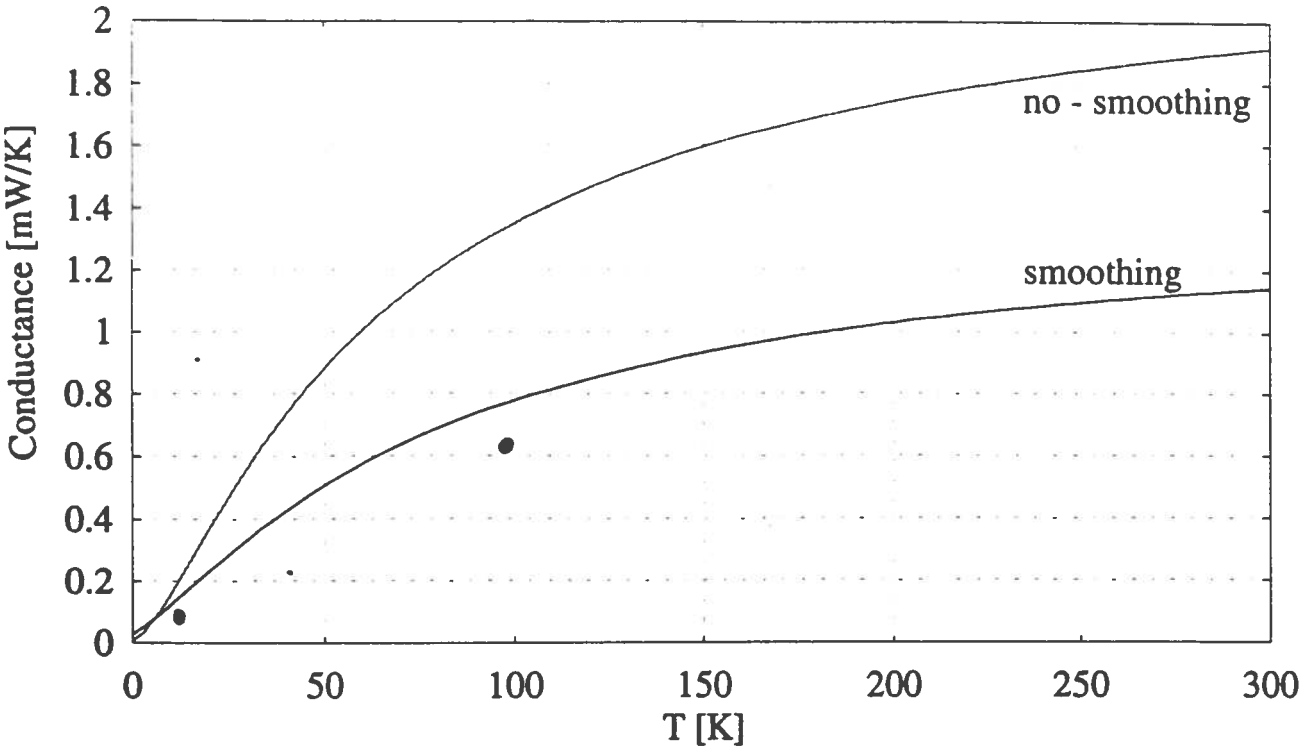

Figure 3: Calculated conductance of the supporting system (lines). Measured conductance (points)

as conduction section the geometric one with discontinuities when passing from materials with different sections. The "smoothing" section is calculated considering a linear smoothing between two consecutive sections of the supporting system. This approximation take in account that the heat flow lines do not follow the geometrical profile of the conductor but tend to smooth the geometrical profile discontinuities. Since there are various big discontinuities in the sections, the calculation with the "smoothing" approximation seems to fit better the effective conductance of the supporting system (see fig 3). In order to check the calculation of the loss, two measurements have been carried out by sending a small amount of power (about 10 - 20 mW) without any sample: the temperature difference of the two heat sinks allowed to determine the thermal conductance of the support. The agreement between the measured values and the "smoothing" curve looks very good, within 0.2 - 0.3 mW/K.

4.2 Convective Losses

A bad vacuum into the conductimeter chamber affects the heat flowing through the sample. According to a simple model, the heat transferred (per unit surface) by conduction through a gas at low pressure P between two surfaces at T_1 and T_2 temperature is given by[16]:

$$\dot{Q} = cost \;\; a_0 \;\; P \;\; (T_2 - T_1) \qquad (W/m^2) \tag{22}$$

where:

$$\begin{aligned} cost &= typical\ gas\ constant\ (2.1\ for\ He\ gas) \\ a_0 &= geometric\ factor \\ P &= gas\ pressure(Pa) \end{aligned}$$

This formula describes the heat transfer for low pressure gases, when the mean free-path l of a molecule is much greater than the dimension of the vacuum chamber d (e.g. $l \gg d$), and the value of 2.1 for the constant is the He typical value.

In fig. 4, the power loss for different level of vacuum versus the sample mean temperature in the two cases for shield temperature of 4.2 K (for He) and 77.3 K (for N) is plotted, given a geometric factor as $a_0 = 0.5$ [16] (for our sample typical dimension). As shown at operating pressure of $10^{-6} - 10^{-5}$ mbar these kind of loss can be neglected. At higher pressure the relation (22) is not any more valid because the mean free-path of a molecule become comparable with the dimensions of the conductimeter. When $P \geq 10^{-4}$ $mbar$ the convective losses can affect heavily the measurements.

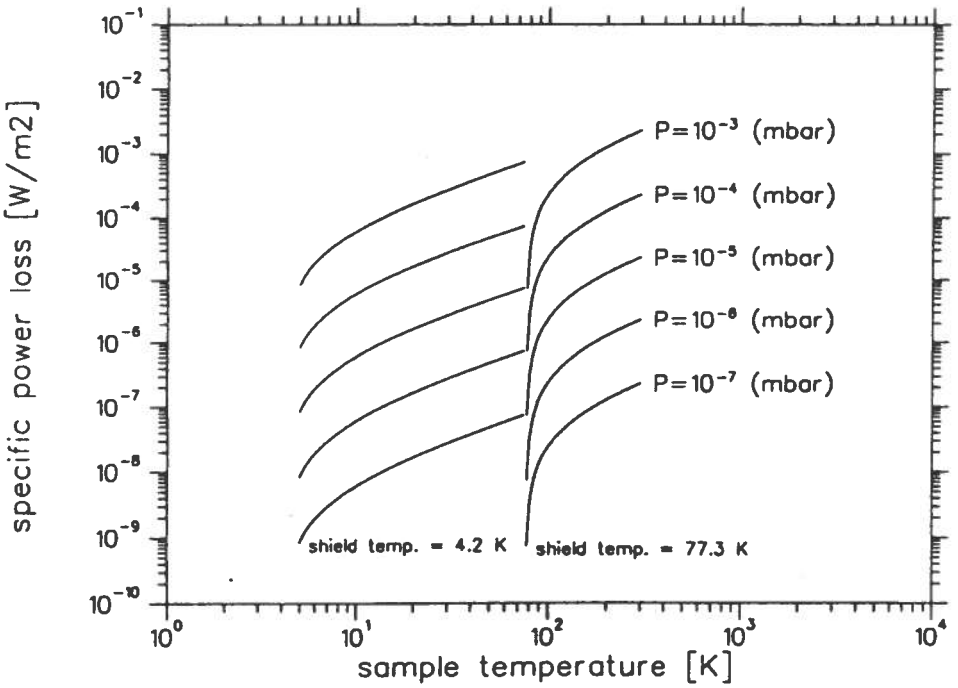

Figure 4: Power loss per unit surface for convection vs. pressure in the conductimeter for different sample temperatures when the shield is at 77.3 K

4.3 Radiative Losses

Because of the T^4 behaviour, the radiation losses usually are negligible below 20 K but become very important when T is the temperature of the liquid nitrogen. Many models describe the radiation heat transfer between two surfaces at different temperature [17], depending on the geometry of the surfaces between which the exchange occurs. The configuration that seems to fit better our geometry is that of two generic shaped surfaces, the greater (the thermal shield) enclosing completely the smaller (the sample). In this case the power radiated by the surface at temperature T_1 toward the other surface at temperature T_2, if the surface of the shield is much larger than the sample one is

$$\dot{Q} = S\,\varepsilon\,\sigma\,(T_2^4 - T_1^4) \qquad (W) \tag{23}$$

where:

ε = surface emissivity, $\sigma = 5.67 \times 10^{-8}(W/m^2K^4)$ Stefan-Boltzmann constant

A more refined model, taking in account the geometry of the surfaces, when the shield surface cannot be considered much larger than the sample one gives

$$\dot{Q} = \frac{S\,\sigma\,(T_1^4 - T_2^4)}{\frac{1}{\varepsilon_1} + \frac{S_1}{S_2}(\frac{1}{\varepsilon_2} - 1)} \tag{24}$$

where:

ε_1, S_1, T_1 are emissivity, surface and temperature of the sample and ε_2, S_2, T_2 are emissivity, surface and temperature of the shield.

In fig. 5 the radiative losses, according to (23) and (24), are plotted vs. the sample temperature with the following values: $\varepsilon_1 = 0.3, \varepsilon_2 = 0.03, S_1 = 8 \times 10^{-3}$ m^2, corresponding to the surface of the biggest sample that can be measured and $S_2 = 2.2 \times 10^{-3}$ m^2.

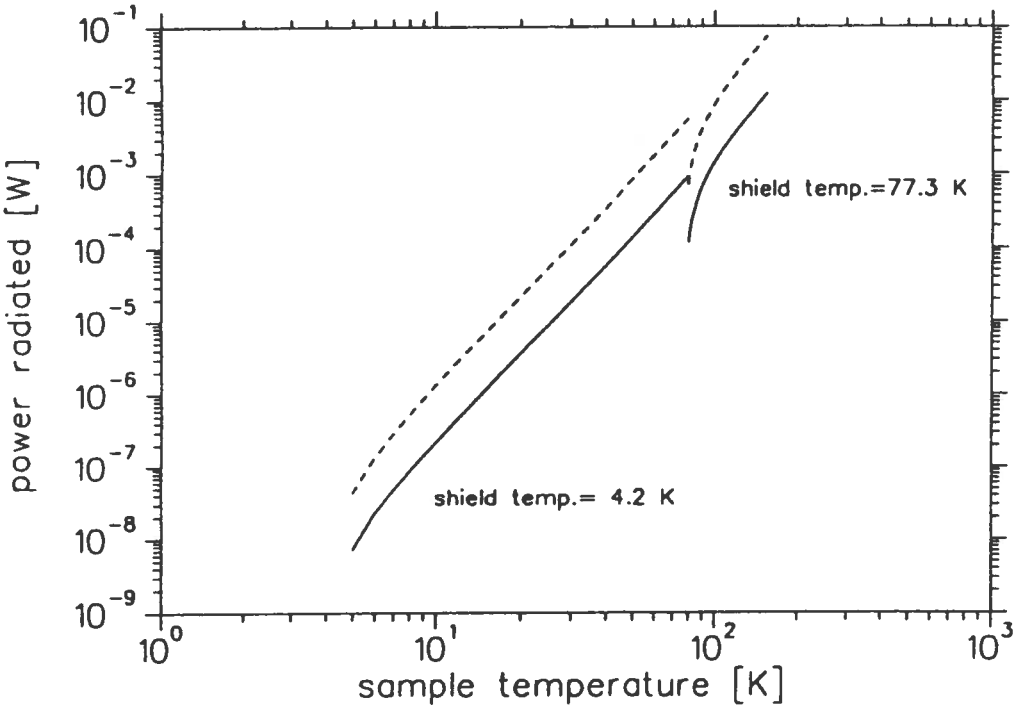

Figure 5: Maximum radiation loss. Dashed lines - relation (23). Solid lines - relation (24)

Fig. 6 shows the radiative losses in term of thermal conductance according to relation (23) with the same parameters.

5 APPARATUS CALIBRATION

The calibration of the apparatus was achieved by measuring the conductivity of a reference material. A *tungsten NIST SRM (Standard Reference material)* sample with diameter of 3.2 mm and length of 50 mm, was used with 3 temperature sensors ($AuFe/KP$ thermocouples) along it. A good thermal contact between the thermocouples and the sample was achieved by 3 copper rings, in contact with the sample, with the temperature sensors fixed in them. For the measurement of the tungsten and for all the other materials the temperature sensors were placed both along the sample, and on the two heat sinks, in order to have the effective temperature gradient along the sample, without the contribution of the surface contact resistance between the sample and the heat sinks.

In fig. 7 the measured values, evaluated with the DAM method together with the certified curve are plotted. The data were obtained in many runs of measurements collected in three years of operation of the conductimeter. As we can see, the agreement is reasonable and good repeatibility, is achieved.

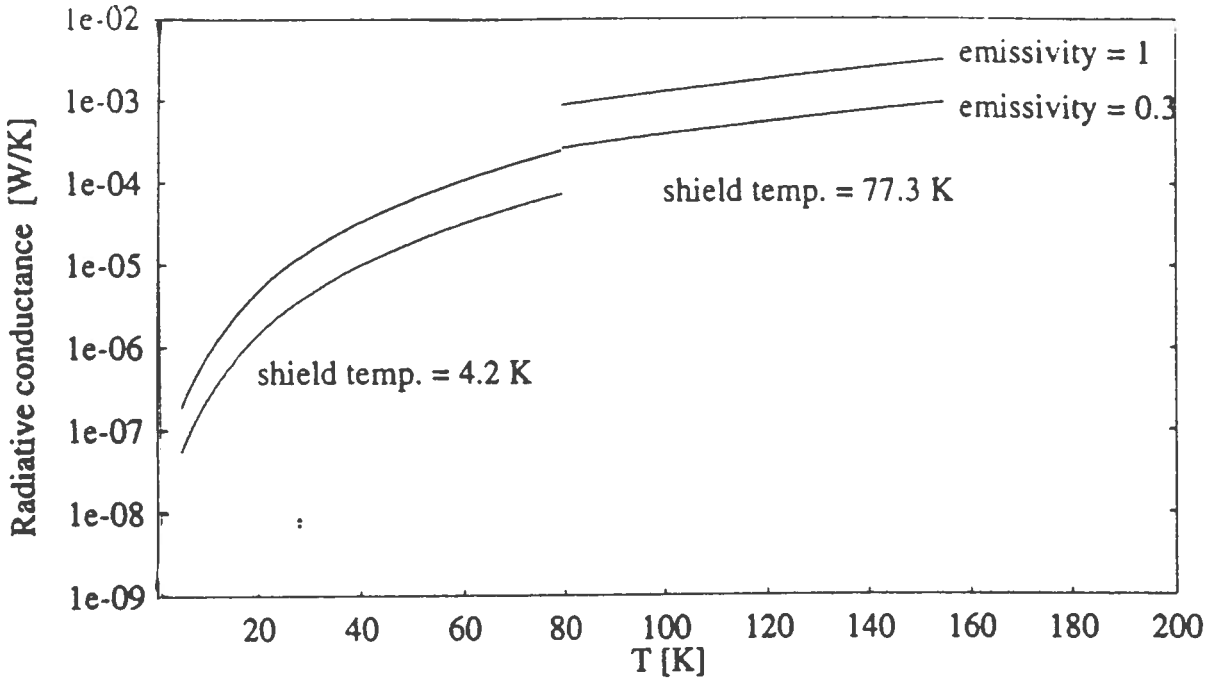

Figure 6: Equivalent conductance of the radiative losses

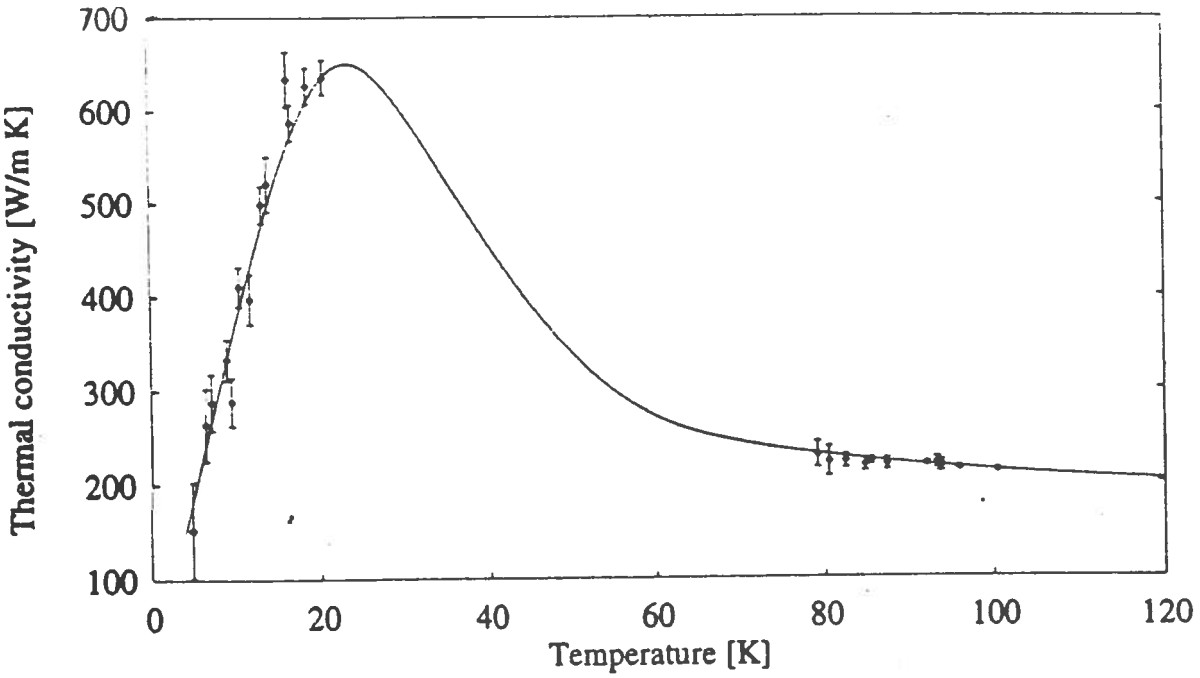

Figure 7: Tungsten thermal conductivity determined with the DAM method. The solid line is the NIST reference curve

In fig. 8 the data obtained with the DAM, the thermal conductivity determined with a polynomial fit of the fourth order is plotted, together with the reference curve. The fourth order fit is the method that better reproduces the behaviour of the thermal conductivity, while an exact application of the TCI method using a power serie of higher order does not reproduces at all the experimental data, as previously said.

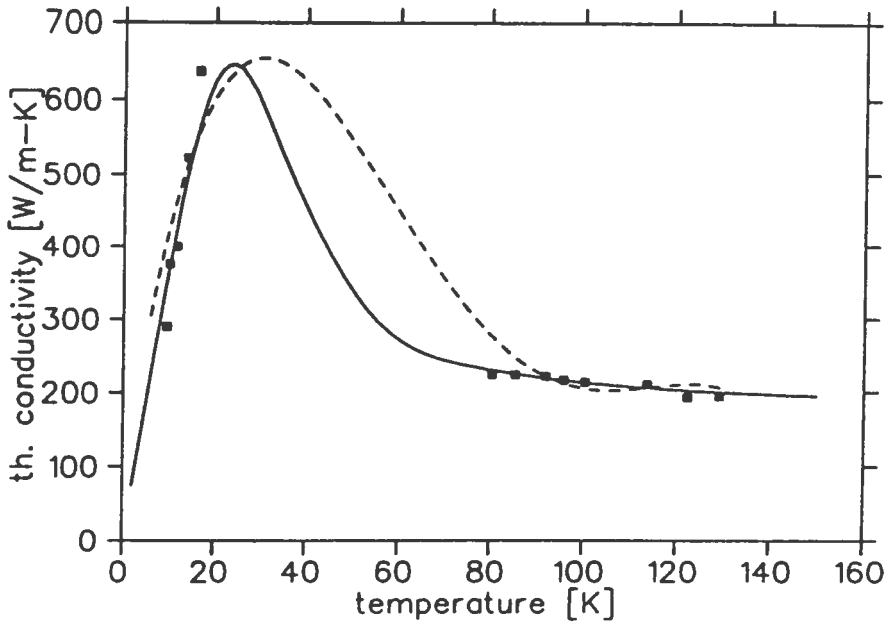

Figure 8: Dashed line - Tungsten thermal conductivity determined with the TCI fitting, using an expansion to the fourth order. Solid line - reference curve. Points - Experimental data with DAM.

6 MEASUREMENTS ON COIL BLOCKS

Some measurements have been carried out on coil blocks cut from real coils, wound with $NbTi$ and Nb_3Sn, conductors. For Nb_3Sn a block cut out from a coil wound with a rectangular cable was measured too. The thermal contact between the heat sinks and the sample was improved by fine machining of the surfaces and by covering them with the high conductivity grease.

6.1 $NbTi$ Magnet

The sample used for this measurements has been cut from $NbTi/Cu$ coil wound with a round wire of 0.5 mm diameter, with stabilizing factor of $Cu : NbTi = 1.35$. The magnet was a solenoid named "LASA1"[18], built in our laboratory to study the dynamic of the quench propagation. The measurements on the $NbTi$ coil block, compared with the conductivity curve calculated with a simple analytical model from the thermal conductivities of its components, are shown in fig. 9.

Unfortunately a mechanical fracture in the sample did not allow to get more data.

6.2 Nb_3Sn Magnets

For Nb_3Sn measurements two different samples have been used, cut from two different coils, named "LASA3"[18] and"LASA5"[18]. The cable used to wind the two coils was the same; it has been produced with the "bronze route" by Vacuumschmelze (D), and is stabilized with an inner copper

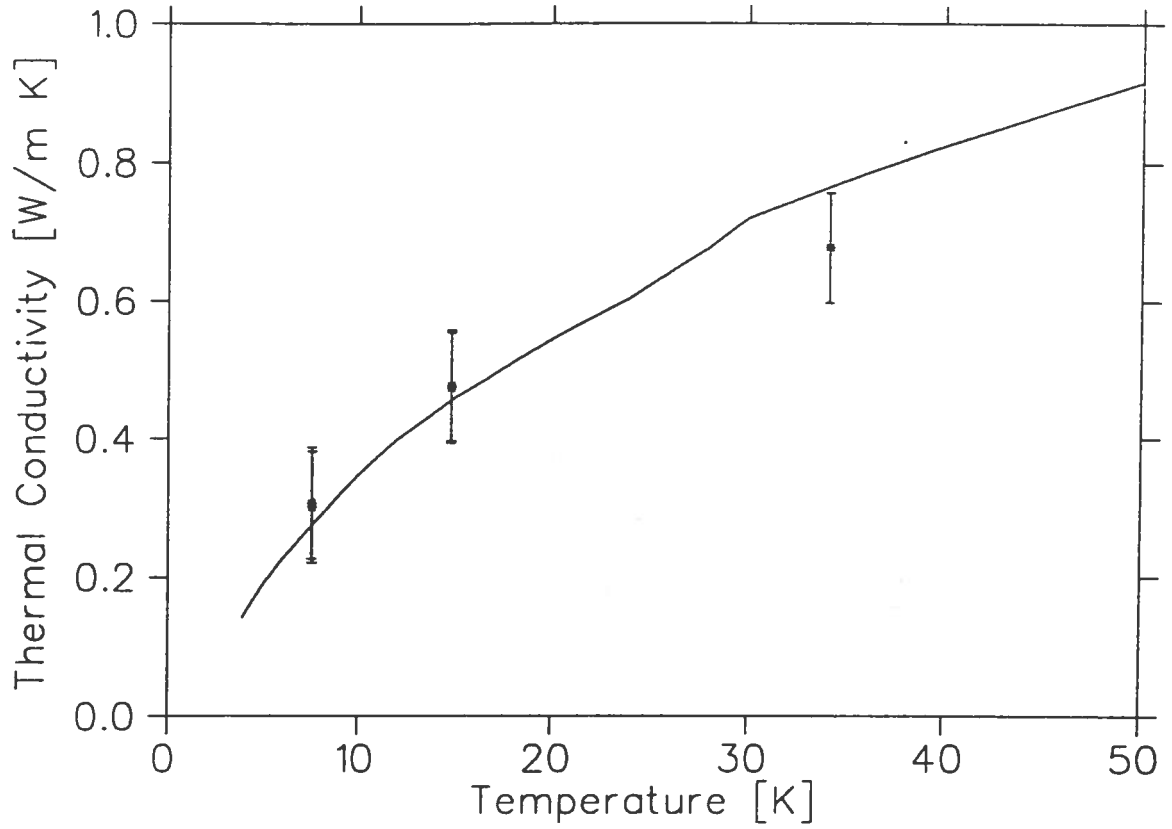

Figure 9: Transverse thermal conductivity of a $NbTi$ coil. Solid lines - Calculated values.

core, protected by a Tantalum barrier, around which there are 6156 Niobium filaments. The insulating "E" glass braid was provided by Vacuumschmeltze too. The coil was built, like all the Nb_3Sn coils, with the "Wind and React" technique. A considerable amount of carbon in the insulation can be inferred, by the gray colour of the coils, caused by the decomposition of the insulation during the reaction procedure. The carbon can increase the thermal contact resistance between turns and can reduce the bonding of the resin to the glass, such to decrease the thermal conductivity of the coil block. The wire is 0.7 mm in diameter, the percentage of the pure copper is 17% of the wire cross section. The braid thickness is 0.075 mm impregnated under vacuum with a two component epoxy resin 3M SCOTCHCAST 280.

6.2.1 Measurements on LASA3

The sample from "LASA3" was a cylinder of 35 mm diameter and 37 mm height obtained by a coaxial milling of the solenoid. During the preparation of the sample some windings flaked off, because of a non perfect impregnation of the conductor with the insulation. Fig. 10 shows the measured value of λ, evaluated with the DAM method, together with the predicted theoretical values, calculated with the same technique used to evaluate the conductive losses in the support of the conductimeter (see section (4.1)).

In fig. 11 the experimental data, fitted with the curve (25) are shown, on an amplified scale.

$$\lambda(T) = 97.6 + 0.1T - \frac{233.5}{T} - 30.4\exp(-\frac{(T-68.4)^2}{1229.7}) \qquad (25)$$

The big difference between the measured and the calculated values depends on the fact that actually the heat can flow along the wire which contains a not negligible part of high purity annealed copper with an electric $RRR \sim 200 - 400$.

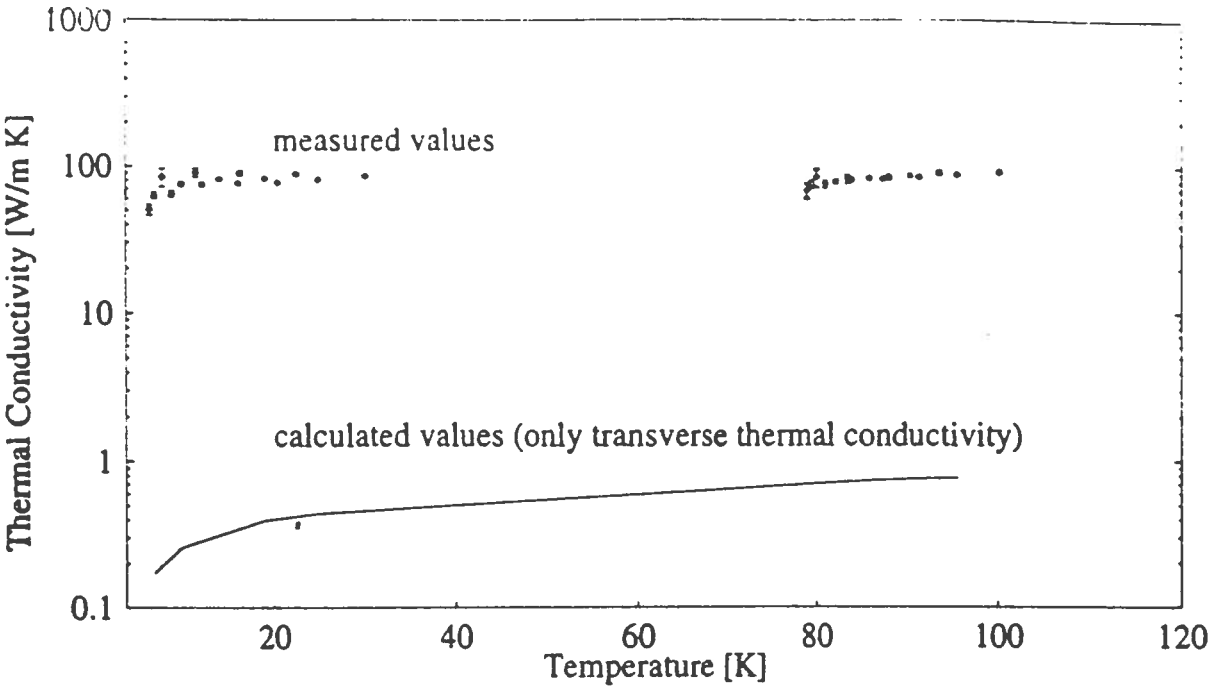

Figure 10: Measured conductivity of LASA3 Nb_3Sn coil. The solid lines is the predicted thermal conductivity according to a theoretical model of the cable of the pure transverse thermal conductivity.

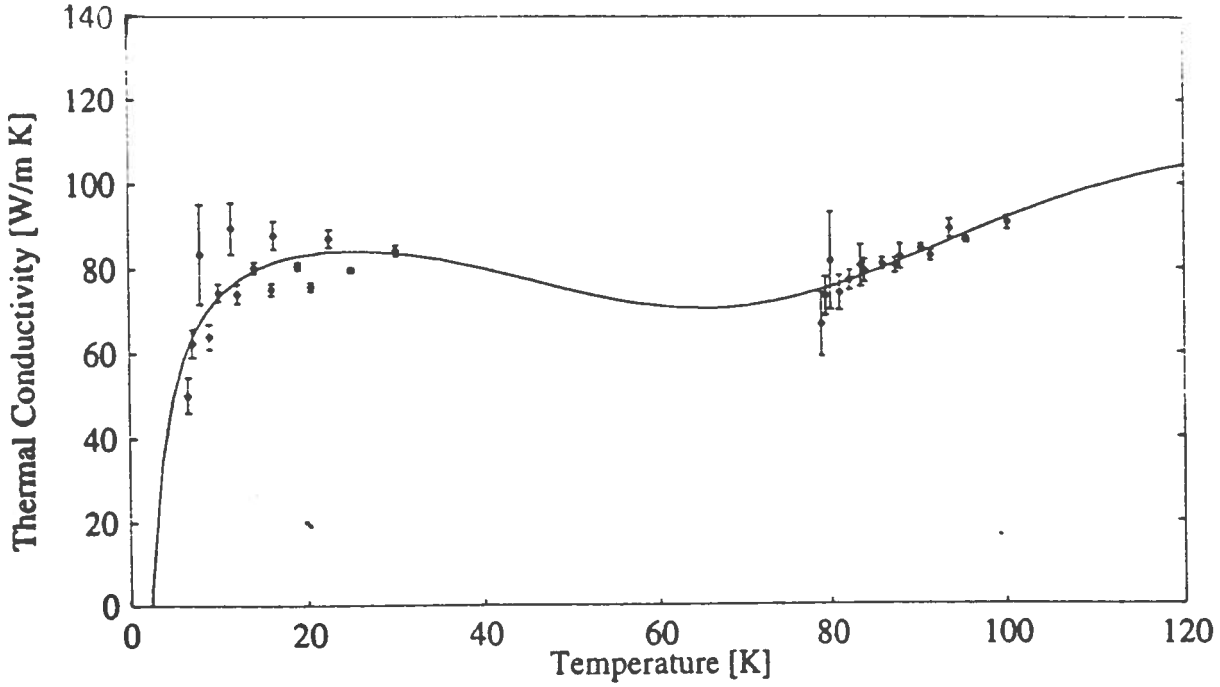

Figure 11: Measured conductivity of LASA3 Nb_3Sn coil.

6.2.2 Measurements on LASA5

The sample measured was cut out by the "LASA5" Nb_3Sn coil with a radial sector geometry, whose inner and outer radius were 24.5 mm and 50.5 mm respectively, 26 mm heigth, because the large dimension of the coil[18] did not allowed a cylindrical shape to fit the dimension allowances of the conductimeter. Moreover, with this geometry, different values of λ can be expected respect to the previous "LASA3" measurements. In fact although the conductor is the same, in the "LASA5" sample there is no continuity of the turns, being cut radially, while in the "LASA3" sample the heat flows along the wire. Fig. 12 shows the experimental data obtained by the DAM method on "LASA5" compared with the calculated values with the same method as for LASA3. In fig. 13 the LASA5 experimental data (DAM method) fitted with the curve (26) together with the data evaluated with a third order polynomial fitting are shown.

$$\lambda(T) = -30.14 \times 10^{-3} + 3.65 \times 10^{-3}T + 0.1\ln(T) + 2.075 \times 10^{-8}T^3 \qquad (26)$$

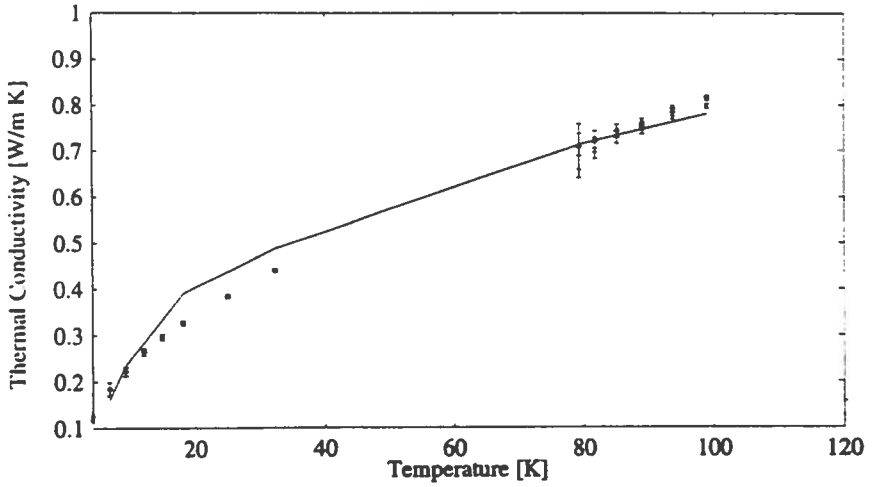

Figure 12: Measured conductivity of LASA5 Nb_3Sn coil. The solid lines is the predicted thermal conductivity according to a theoretical model of the cable.

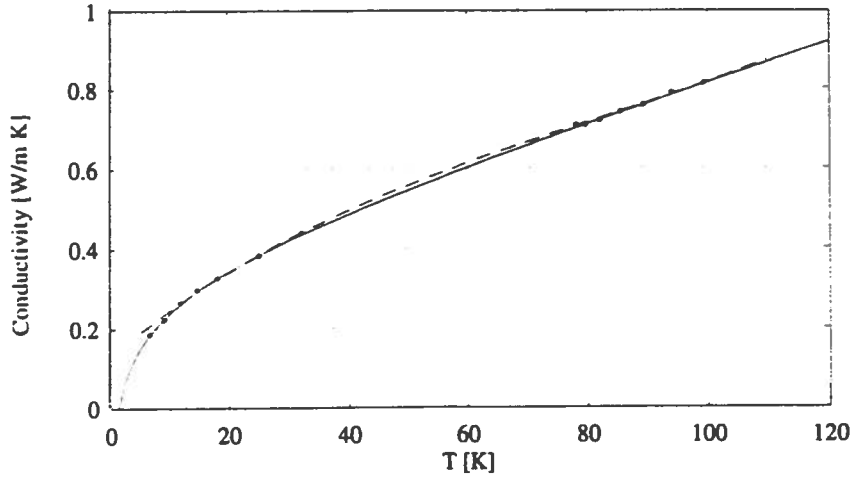

Figure 13: Measured conductivity of LASA5 Nb_3Sn coil. Solid line eq.(26). Dashed line - thermal conductivity determined with TCI fitting using an expansion to the third order.

6.2.3 Observation on the LASA3 and LASA5 Nb_3Sn Measurements

Comparing the data obtained with "LASA3" and "LASA5" coils we can see that the measured thermal conductivity is quite different, even if the windings are the same. This is due to the different preparation of the samples which for the LASA3 sample gave the value of the longitudinal conductivity, dominated by the high conductivity copper used for stabilization. This is confirmed by the behaviour of the thermal conductivity showing a maximum around the 20 - 30 K, that is typical of pure metals (see fig 11). Conversely in the measurements of "LASA5" the real transverse (i.e. turn to turn) thermal conductivity has been measured.

6.2.4 Measurements on Nb_3Sn Rutherford cable

The sample was obtained by a block of coil of the SOLEMI 2 solenoid, one of the solenoid composing the SOLEMI facility at LASA Lab.[19]. The sample was a rod of 43 mm height and 14 mm diameter. For a second run of measurements the sample diameter was reduced, by milling, to 8 mm in order to decrease its conductance, providing in this way a higher temperature gradient along the sample. The measured data together with the calculated values, with the same model as *NbTi* measurements, are shown in fig. 14.

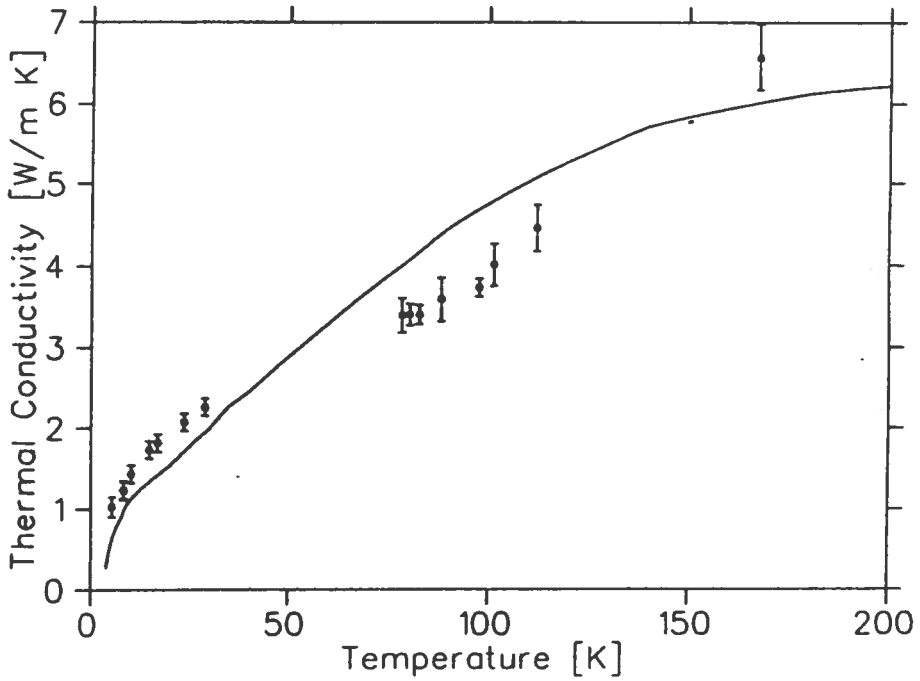

Figure 14: Measured conductivity of SOLEMI2 Nb_3Sn coil block. Solid line - Calculated values

7 B1-2212 HIGH T_C SUPERCONDUCTOR

The sample measured was a rod of Bi-2212 (Bi_2-Sr_2-Ca-Cu_2-O_8) whose nominal critical temperature was 85 K. BSCCO is important for magnet technology because it can be used for winding solenoid for high magnetic field ($\geq$ 20 T). Furthermore solid rods of Bi-2212 are going to be used as main elements of current leads for superconducting magnets of cryogenic apparata. The sample has been manufactured by Hoechst (D) and was given to us by CERN [20], where a project for a current lead based on HT_c superconductor is under development. The sample diameter was 5 mm and its height was 32 mm In fig. 15 the measured values, together with the curve given by the manufacturer is

shown. The solid line is the interpolation od the experimantal data according to the relation:

$$\lambda(T) = 0.58 + 0.09T - 1.2 \times 10^{-4}T^2 - 8.48\left(\frac{1}{1 + \exp\left(-\frac{T-72.94}{31.01}\right)}\right) \tag{27}$$

The difference between the measured data and the curve given by the manufacturer is due to the fact that the given curve is only a reference curve of the material, not the certification of the thermal conductivity of that particular sample. Moreover the same ceramic compound can have different physical properties if subjected to different thermo-mechanical processes, during the manufacturing. For these reason we are confident that the measured thermal conductivity of Bi-2212 are the real value for that particular sample. In fig. (16) a picture showing all the samples described in the paper is reported.

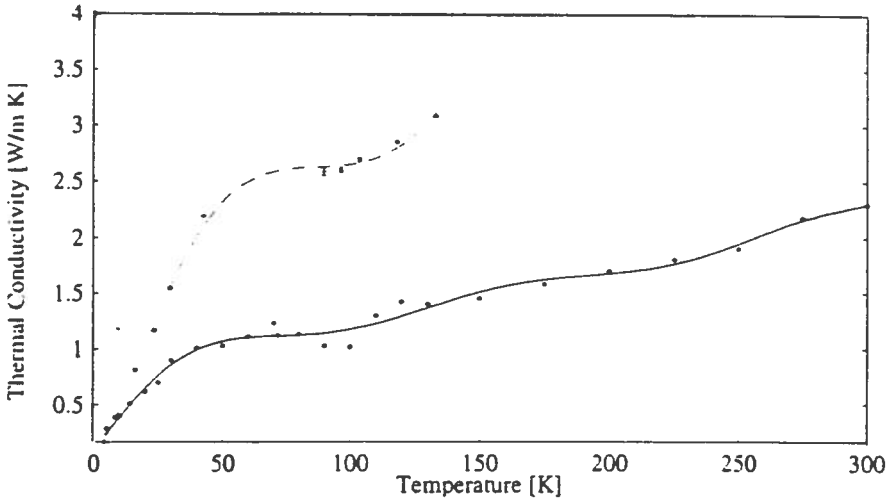

Figure 15: Measured conductivity of Bi-2212 rod. Solid line - reference curve. Dashed line - relation (27).

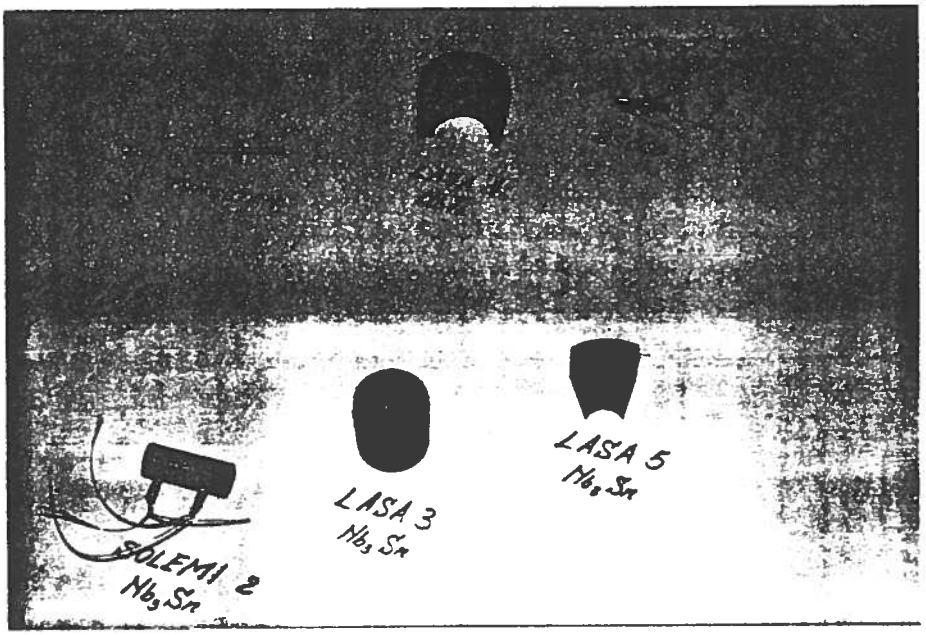

Figure 16: All the samples described.

8 CONCLUSION

The measuring apparatus shows good performances, as from the tungsten calibration. Convective losses can be neglected, because the routinely operation pressure is lower than 10^{-5} mbar. Radiative losses must be considered when operating at liquid nitrogen temperature and samples of big dimensions. The parasitic conductance of the supporting system must be taken in account when measuring samples with conductance smaller than 2 - 3 mW/K. The apparatus has the capablilty to measure samples with thermal conductance in the range 0.5 - 50 mW/K with an accuracy of about 5%. As for the measurements of the coil blocks, difference between the behaviour of the LASA3 and the LASA5 samples indicates the strong contribution of the longitudinal conductance to the effective transverse conductance. This imply that the sample perparation is very important and leads to measure different properties. We found the direct measurements of the thermal conductivity of the windings very useful for the prediction of the stability and quench behaviour in superconducting magnets.

9 Acknowledgements

We are grateful to Mirko Pojer and Daniela Bettinelli for their help in taking the data.

References

[1] E. Acerbi, F. Alessandria, G. Baccaglioni, C. Birattari, E. Fabrici, L. Rossi, A. Sussetto, "High field superconducting solenoid for the LASA in Milan," *IEEE Trans. on Mag.* , Vol.24, No.2, March 1988, pp. 1417-1420.

[2] J.E.C. Williams, S. Pourrahimi, Y. Iwasa, L. J. Neuringer, "600 MHz spectrometer magnet," *IEEE Trans. on Mag.,* , Vol.25, No.2, March 1989, pp.1767-1770.

[3] P. Turowski, Th. Schneider, "19.3 T with a superconducting magnet," *IEEE Trans. on Mag.,* Vol.24, No.2, March 1988, pp.1063-1066.

[4] A. Ishiyama and Y. Iwasa, " Quench propagation velocity in an epoxy-impregnated Nb_3Sn superconducting winding model," *IEEE Trans. on Mag.,* Vol. 24, No.2, March 1988, pp. 1194-1196

[5] C.H. Joshi and Y. Iwasa, "Prediction of current decay and terminal voltages in adiabatic superconducting magnets," *Cryogenics,* 1989 Vol.29 March, pp.157-167.

[6] E. Acerbi, G. Baccaglioni, M. Canali and L. Rossi, "Experimental study of the quench properties of epoxy impregnated coupled coils wound with NbTi and Nb_3Sn ", *IEEE Trans. on Mag.,* Vol. 28, No.1, january 1992, pp. 731.

[7] M.N. Wilson, *Superconducting Magnets,* Clarendon Press Oxford 1983, p. 208

[8] R.P. Reed and A.F. Clark, *Materials at low temperatures,* American Society for Metals, 1983, pp.133-161.

[9] J.E. Jensen, R.B. Steward, W.A. Tuttle, *Selected Cryogenic Data,* Bubble Chamber Group of Brookhaven Nat. Lab., Nov. 1966, section VII.

[10] H. Bougrine, M. Ausloos, "Highly Sensitive Method for Simultaneous Measurements of Thermal Conductivity and Thermoelectric Power: Fe and Al examples, *Rev. Sci.Instrum.* **66 (1)**, 199 (1995).

[11] F.Menotti, *"Misure ed Analisi della Conducibilita' Termica in Superconduttori e Materiali Compositi a Basse Temperature"* thesis at University of Milan 1995.

[12] J. G. Hust, A. B. Lankford, "International Journal of thermophysic", Vol.3, No.1, 67-77.

[13] F. Broggi, S. Piuri, L. Rossi, An Apparatus for Thermal Conductivity Measurements at Cryogenic Themperature on Coil Blocks." I.N.F.N. Report INFN/TC - 93/01 26/MarzoO/1993.

[14] J.C. Hust, P.J. Giarratano, "Thermal conductivity" in *Semi - annual Technical Report on Material Research in Support of Superconducting Machinery,*NBSIR 74-359,1974a,Nat. Bureau of Standards, pp. 29-44.

[15] C.Barrila', F. Broggi, L.Rossi, G.Volpini, "Measurements of Thermal Conductivity of Epoxy Impregnated $NbTi$ and Nb_3Sn Windings", *IEEE Trans. on Mag.,* Vol.28, No.1, January 1992, pp.900-903.

[16] Guy K. White, "Experimental techniques in low-temperatures physics", Claredon Press Oxford 1987, pp. 127-131.

[17] R. Siegel, J. R. Howell, "Thermal radiation heat transfer", International Student Edition, McGraw Hill Kogakusha 1972, p. 243 and p. 787.

[18] G. Baccaglioni, M. Canali, G.C. Cartegni, C. Fumagalli, M. Fusetti, L. Gini, L. Grilli, A. Leone, "Costruzione di Solenoidi Superconduttori con Campo di 10 Tesla, presso Il Laboratorio L.A.S.A., Per Studi Di Transizione dallo Stato Superconduttivo a quello Resistivo." I.N.F.N. Report INFN/TC - 92/95 7/Ottobre/1992.

[19] E. Acerbi, G. Baccaglioni, L. Rossi, G. Volpini, M. Biltcliffe, P. Daniels, J. Mellors, K. Timms, " Design and Experimental Results of the Nb_3Sn Double Insert for an 18 Tesla, 100 mm Free Bore Solenoid." Presented at MT - 14 Conference, Tampere (Finland)m June 1995, to be published in the Proceedings.

[20] A.Ballerini, CERN, AT/MA, *private communication.*